Quantization effect on capacitancevoltage and currentvoltage characteristics of an InAs/AlSb/GaSb interband tunneling diode

L. Yang, M. C. Wu, J. F. Chen, Y. K. Chen, G. L. Snider, and A. Y. Cho

Citation: Journal of Applied Physics **68**, 4286 (1990); doi: 10.1063/1.346222
View online: http://dx.doi.org/10.1063/1.346222
View Table of Contents: http://scitation.aip.org/content/aip/journal/jap/68/8?ver=pdfcov
Published by the AIP Publishing

Quantization effect on capacitance-voltage and current-voltage characteristics of an InAs/AlSb/GaSb interband tunneling diode

L. Yang, M. C. Wu, J. F. Chen, Y. K. Chen, G. L. Snider,[a] and A. Y. Cho
AT&T Bell Laboratories, Murray Hill, New Jersey 07974

(Received 18 January 1990; accepted for publication 25 June 1990)

Capacitance-voltage measurements were performed on the InAs/AlSb/GaSb interband tunneling diode at various frequencies. Theoretical analyses using a self-consistent Schrödinger–Poisson solver were found in agreement with the experimental results under the forward-bias condition. The quantization energy of each subband of the electron in the InAs accumulation region is used to predict the tunneling current cutoff voltage in agreement with that of the current-voltage measurements. Therefore, the cutoff of the interband tunneling process is mainly caused by the crossover of the electron subband energy in the InAs conduction band with respect to the valence band of the GaSb electrode due to the increased external bias voltage.

I. INTRODUCTION

Recently, much interest was drawn on the use of the InAs/AlSb/GaSb material system in the application of tunneling diodes which produce negative differential resistances (NDR).[1–10] In these devices, the operation mechanism bases on the unique feature that the conduction-band minimum of InAs is lower than the valence-band maximum of GaSb by 0.15 eV.[11] A peak-to-valley current ratio (P/V ratio) as high as 20 at room temperature was achieved using the InAs/AlSb/GaSb/AlSb/InAs resonant interband tunneling structure.[4] In Ref. 10, we reported the InAs/AlSb/GaSb single-barrier interband tunneling diode. A P/V ratio of 4.7 at room temperature was obtained with an AlSb barrier thickness of 15 Å. In previous works, only current-voltage (I-V) characteristics were shown because the capacitance-voltage (C-V) measurement could not be performed on these highly conductive devices (with a typical current density of 1 kA/cm^2). In this work, we fabricated an InAs/AlSb/GaSb single-barrier interband tunneling diode with an AlSb barrier thickness of 50 Å. Because of a thick barrier layer to impede a significant interband tunneling process, the conduction is low enough to allow an accurate C-V measurement. A theoretical analysis using a self-consistent Schrödinger–Poisson solver was performed and the calculated capacitances were found in agreement with the experimental data under the forward-bias condition. In the same calculation, the quantization energies of the subbands in the InAs accumulation region were obtained. It is found that the theoretical predicted valley-current voltage, 0.05 V, agrees with the experimental I-V characteristics.

II. DEVICE FABRICATION AND CHARACTERIZATION

The structure of the InAs/AlSb/GaSb tunneling diode shown in Fig. 1 was grown by molecular-beam epitaxy (MBE)[12] on a GaAs (100) n^+ substrate. The detailed growth condition was reported in Ref. 10. After the growth of a 0.5-μm-thick n^+ InAs buffer layer, a 50-Å-thick undoped GaSb, a 50-Å-thick undoped AlSb, a 50-Å-thick undoped InAs, and a 800-Å-thick p^+ GaSb contact layer were subsequently grown. The n^+ InAs layer was doped by Si with a doping concentration about 1×10^{18} cm^{-3}. The p^+ GaSb layer was doped by Be with a doping concentration about 5×10^{18} cm^{-3}. The diode with a 60 μm diam was fabricated by Au/Be/Ti/Au contact metalization, followed by a wet chemical mesa-isolation etching using the metal as a etching mask.

The band diagram of the single-barrier InAs/AlSb/GaSb tunneling diode with a small external bias is shown in Fig. 1(a). At this point, because there are unoccupied states in the valence band of GaSb, the electrons in InAs can tunnel through the AlSb barrier layer into GaSb. However, when the external bias is further increased, the first subband energy of the electron in the triangular well is raised above the valence band of GaSb. Then, the tunneling process is impeded. Figure 2(a) shows the room-temperature I-V characteristics of the device with an AlSb barrier layer thickness of 50 Å. For the purpose of comparison, the I-V characteristics of a similar device but with a 15-Å-thick AlSb barrier layer[10] is also shown in Fig. 2(b). It can be seen that the interband tunneling probability is greatly reduced by using a thick AlSb barrier layer. The forward turn-on voltage of the diode is about 0.5 V. The I-V curve between 0.3 and 0.6 V exhibits an ideality factor of 2.2 as seen in the conductance plot in Fig. 2(a). Below 0.3 V, we observe two negative slope regions in the conductance plot. One occurs near 0.05 V and the other occurs near 0.3 V. The first negative slope corresponds to the cutoff of the interband tunneling process due to the external bias, as suggested by the I-V curve in Fig. 2(b). Because the tunneling current is smaller compared with other current paths (e.g., the minority-diffusion currents), the cutoff tunneling current only results in a negative slope in the conduction plot in Fig. 2(a). However, for the device with a thinner AlSb barrier layer shown in Fig. 2(b), the tunneling process dominates the current conduction, the

[a] Present address: ECE Department, University of California, Santa Barbara, CA 93106.

 0021-8979/90/204286-04$03.00

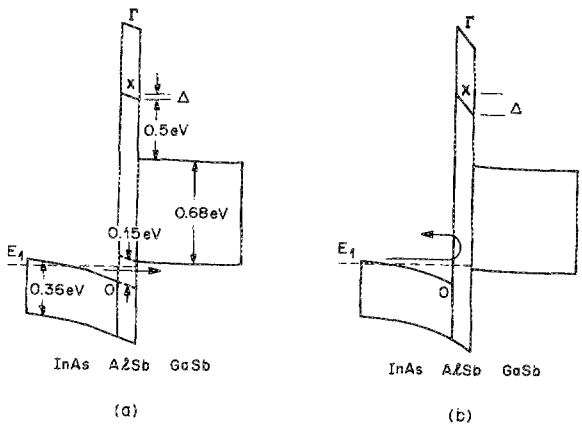

FIG. 1. Band diagrams of an InAs/AlSb/GaSb single-barrier tunneling diode at a bias of (a) 0.02 V and (b) 0.06 V.

cutoff of the tunneling current results in a negative differential resistance region with a peak-to-valley ratio of 4.7.

The mechanism for the second negative slope in the conduction plot is not well understood at this moment. However, it is believed that this effect is unlikely due to the variation of the AlSb barrier thickness. We speculate that this process may be similar to that of a InAs/AlGaSb/InAs single-barrier tunneling diode.[5] In this process, because of the small band gap of InAs, the imaginary propagation constant in the forbidden band of InAs needs to be calculated by the two-band $k\cdot p$ method which again could result in an NDR in the I-V characteristics as observed in Ref. 5. We are not able to confirm this speculation with a theoretical calculation at this moment because a simple Wentzel–Kramers–Brillouin (WKB) approximation would not apply to this complicated band diagram.

The low conduction of the tunneling diode with a thick AlSb barrier layer permits an accurate capacitance-voltage measurement. The diode was probed by a Cascade probe, and the impedance was measured by HP 8720A network analyzer. The measurements were performed with frequencies of 130 MHz, 400 MHz, and 1 GHz. After the correction of the series contact resistances ($\sim 4\ \Omega$ in our case mostly from the probe/substrate contact), almost identical capacitance-voltage curves for difference frequencies were obtained as shown in Fig. 3.

In the forward-bias condition, the capacitance first increases linearly with the bias and then begins to saturate to ~ 27 pF after 0.5 V. Under the forward-bias condition, both electrons in the InAs side and the holes in the GaSb side accumulate at the AlSb heterointerfaces. However, unlike what is usually seen in the C-V curve of a Si/SiO_2 capacitor, the capacitance does not saturate to a constant as soon as the accumulation occurs. This is because the width of the wave packet of the bound electrons in the triangular well at the InAs/AlSb interface is comparable to or even wider than the AlSb barrier thickness. Therefore, numerical calculation of the electron distribution in the triangular well is needed to interpret the experiment data.

In the electrostatic potential analysis, the heavy hole plays a much more important role than the light hole which was first treated by Esaki, Chang, and Mendez[9] using the Fermi–Thomas approximation. Because of a large effective density of states of the valence band of the heavy hole, the

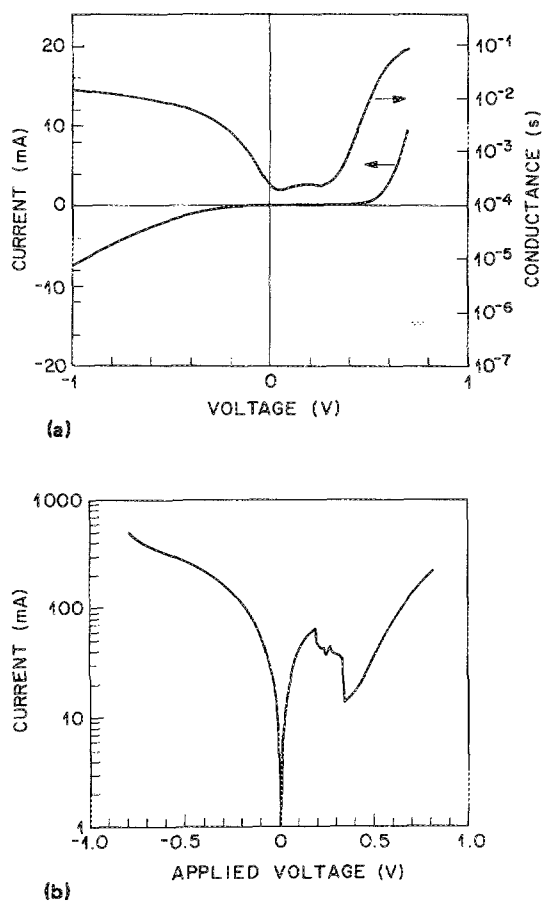

FIG. 2. (a) The current and the differential conductance as functions of the applied voltage of an InAs/AlSb/GaSb single-barrier tunneling diode with a 50-Å AlSb barrier. (b) The current-voltage characteristics of tunneling diode with a 15-Å AlSb barrier.

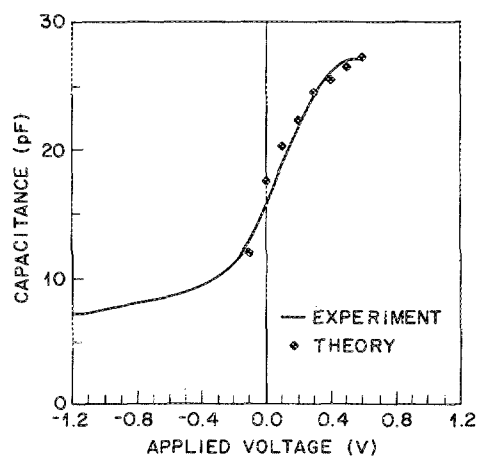

FIG. 3. Measured (—) and calculated (■) capacitance-voltage characteristics. The calculation was done using a Schrödinger–Poisson solver. The carriers with a sheet concentration of 3.7×10^{12} cm^{-2} accumulate at the interfaces at 0.6 V.

band bending in the GaSb side is much smaller than that of the InAs side, as verified by the computer self-consistent Schrödinger–Poisson solver at 0.6 V. Therefore, in our analyses, the band bending in the GaSb side under the accumulation condition is neglected for simplicity, and all the external bias is assumed to drop across the undoped AlSb barrier and the InAs layer. In calculating the quantized states in the triangular well formed by the AlSb barrier and the bent InAs region, we make the following assumptions. First, we assume that all the donor states with energies lower than the Fermi level are occupied. Second, we assume the effective mass approximation is still valid because we expect the quantization energy would be large due to a very small electron effective mass ($0.023\,m_e$). These simplifications greatly ease the calculation effort. All the physical parameters such as dielectric constants, effective masses are taken from Ref. 13. The band overlap of the InAs/GaSb system is assumed to be 0.15 eV. The nominal thickness of the AlSb barrier is used. Because the potential barrier formed by AlSb is so large that the calculation results are insensitive to the relative band alignment between AlSb and InAs. In this case, we assume the valence-band edge of InAs coincides with that of AlSb. The effect of strain on the band structure is not considered in our calculation.

In our numerical algorithm, the conduction band (or valence band) and the associated bound states are found by solving the Schrödinger and Poisson equations self-consistently in one dimension, using the method of finite differences. The finite difference formulation of Schrödinger's equation leads to a matrix which is real, symmetric, and tridiagonal. The eigenvalues and eigenvectors of this matrix are the solution of the Schrödinger equation, which are used to find the electron and hole concentrations needed to solve the Poisson equation.[14,15] Newton's method is employed to obtain a self-consisent solution of both equations.[16]

Once the carrier concentrations for various bias voltages are obtained by the computer calculation, the capacitance as a function of the applied voltage is readily computed. The calculated capacitances are superimposed on the experimental C-V curve in Fig. 3. It can be seen that a very good quantitative agreement (within 10%) was obtained. The linear increase of capacitance with the applied voltage is mainly due to the narrowing of width of the electron envelope wave packet. Because of a small electron effective mass, the electron wave packet spreads quite far away from the InAs/AlSb interface. We found that, even at 0.6 V, the peak of the electron envelope function is still about 100 Å away from the InAs/AlSb interface, suggesting that thick spacer layer may be needed to reduce the impurity scattering and to increase the electron coherent length in this type of tunneling structure. For homojunction interband tunneling diode, this type of optimization would not be possible because the doping is the only method to reduce the tunneling barrier between the conduction band and the valence band.

The calculated quantization energies for the first subband and the second subband with the minimum conduction-band edge of InAs in the triangular well as the energy reference along with the potential drop across the AlSb barrier, Δ, are plotted in Fig. 4. The calculated band diagram is

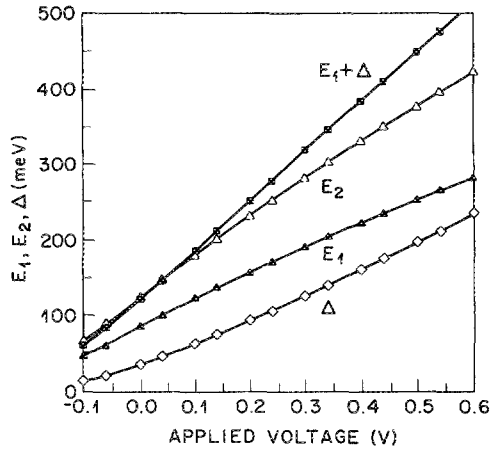

FIG. 4. Subband energies (E_1 and E_2) of the electron in the InAs accumulation region and the potential drop (Δ) across the AlSb barrier layer as functions of the external applied voltage. When $E_1 + (\Delta)$ exceeds 0.15 eV, the interband tunneling process is cutoff, assuming no phonon-assisted tunneling process.

shown in Fig. 1 along with the first subband energy of the electron, E_1, in the InAs triangular well. The sum of E_1 and Δ indicates the energy difference between the first subband of the electron in InAs and the valence band of GaSb. It can be seen that with a bias of 0.05 V, the first subband of the electron in the InAs accumulation regions begins to exceed the valence band of the GaSb layer. This results in a cutoff of the interband tunneling process. This predicted cutoff voltage agrees with that of the I-V characteristics in Fig. 2(a). For the device with a 15-Å AlSb barrier layer, the predicted cutoff voltage, 0.12 V, is close to the peak-current voltage in Fig. 2(b) after correcting the voltage drop across the external contact resistance (typically 1 Ω).

The discrepancies between the calculated capacitances and the measured capacitances may be further reduced by considering the band bending in the GaSb side. However, the self-consistent Schrödinger–Poisson solver does not yield an accurate result for a barely bound state for hole due to its large effective mass. Therefore, the correction due to the band bending in the GaSb side is not included.

We are interested in extracting the built-in voltage using the C-V data under the depletion condition. The built-in voltage in this case is the band overlap of the InAs/GaSb system. But from the capacitance value at -0.15 V, it seems to suggest an undoped region as thick as 250 Å which is much larger than the nominal thickness of the undoped region (150 Å). The Debye length for InAs with a concentration of 1×10^{18} cm^{-3} is about 50 Å. To extract the built-in voltage from the C^{-2}-V, the thickness of the undoped region needs to be known very accurately. The uncertainty of the undoped layer thickness of our structure would give a very poor accuracy of extracted built-in voltage. However, we notice a monotonic decrease of the capacitance with the reversed bias up to -1 V, indicating that there is no inversion at the InAs/AlSb interface even when the band bending of the InAs layer exceeds its band gap. This seems to suggest that the valence-band edge of AlSb is not likely significantly lower than that of InAs.

IV. CONCLUSION

We have analyzed the C-V data obtained from an InAs/AlSb/GaSb single-barrier tunneling diode. Excellent agreement was obtained between the measured C-V data and the calculated results using a self-consistent Schrödinger–Poisson solver. In addition, from the calculated subband quantization energy of the electron in the InAs accumulation region, we found that the predicted interband-tunneling cutoff voltages agree with the experimental values.

[1]L. F. Luo, R. Beresford, and W. I. Wang, Appl. Phys. Lett. **53**, 2320 (1988).
[2]R. Beresford, L. F. Luo, and W. I. Wang, Appl. Phys. Lett. **55**, 694 (1989).
[3]J. R. Soderstrom, D. H. Chow, and T. C. McGill, Appl. Phys. Lett. **55**, 1348 (1989).
[4]J. R. Soderstrom, D. H. Chow, and T. C. McGill, Appl. Phys. Lett. **55**, 1094 (1989).
[5]R. Beresford, L. F. Luo, and W. I. Wang, Appl. Phys. Lett. **54**, 1899 (1989).
[6]C. Tejedor, J. M. Calleja, F. Meseguer, E. E. Mendez, C. A. Chang, and L. Esaki, Phys. Rev. B **32**, 5303 (1985).
[7]H. Takaoka, Ch.-A. Chang, E. E. Mendez, L. L. Chang, and L. Esaki, Physica **117B**, 741 (1983).
[8]L. F. Luo, R. Beresford, and W. I. Wang, Appl. Phys. Lett. **55**, 2023 (1989).
[9]L. Esaki, L. L. Chang, and E. E. Mendez, Jpn. J. Appl. Phys. **20**, L529 (1981).
[10]J. F. Chen, M. C. Wu, L. Yang, and A. Y. Cho, J. Appl. Phys. **68**, 3040 (1990).
[11]L. L. Chang and L. Esaki, Surf. Sci. **98**, 70 (1980).
[12]A. Y. Cho, Thin Solid Films, **100**, 291 (1983).
[13]S. M. Sze, *Physics of Semiconductor Devices*, 2nd ed., (Wiley, New York, 1981, p. 849.)
[14]K. Inoue, H. Sakaki, J. Yoshino, and T. Hotta, J. Appl. Phys. **58**, 4277 (1985).
[15]S. Laux and F. Stern, Appl. Phys. Lett. **49**, 91 (1986).
[16]F. Hildebrand, *Introduction to Numerical Analysis*, 2nd ed. (Dover, New York, 1987, p. 584).